Cancer Cell
Article

The PAF Complex Synergizes with MLL Fusion Proteins at *HOX* Loci to Promote Leukemogenesis

Andrew G. Muntean,[1] Jiaying Tan,[1] Kajal Sitwala,[1] Yongsheng Huang,[2] Joel Bronstein,[1] James A. Connelly,[1] Venkatesha Basrur,[1] Kojo S.J. Elenitoba-Johnson,[1] and Jay L. Hess[1,*]
[1]Department of Pathology
[2]Center for Computational Medicine and Bioinformatics
University of Michigan Medical School, Ann Arbor, MI 48109, USA
*Correspondence: jayhess@umich.edu
DOI 10.1016/j.ccr.2010.04.012

SUMMARY

MLL is involved in chromosomal rearrangements that generate fusion proteins with deregulated transcriptional activity. The mechanisms of MLL fusion protein-mediated transcriptional activation are poorly understood. Here we show MLL interacts directly with the polymerase associated factor complex (PAFc) through sequences flanking the CxxC domain. PAFc interacts with RNA polymerase II and stimulates posttranslational histone modifications. PAFc augments MLL and MLL-AF9 mediated transcriptional activation of *Hoxa9*. Conversely, knockdown of PAFc disrupts MLL fusion protein-mediated transcriptional activation and MLL recruitment to target loci. *PAFc* gene expression is downregulated during hematopoiesis and likely serves to regulate MLL function. Deletions of MLL that abolish interactions with PAFc also eliminate MLL-AF9 mediated immortalization indicating an essential function for this interaction in leukemogenesis.

INTRODUCTION

MLL is a histone methyltransferase containing a C-terminal SET domain that methylates histone H3 lysine 4, a mark commonly associated with gene activation (Milne et al., 2002; Nakamura et al., 2002; Strahl et al., 1999). MLL is required for normal embryonic development through proper maintenance of patterns of *Hox* gene expression (Yu et al., 1995). MLL also plays a central role in regulating hematopoietic stem cell self-renewal and progenitor expansion (Jude et al., 2007; McMahon et al., 2007). The protein is of particular biomedical importance because rearrangements involving *MLL* located at chromosome 11q23 are one of the most common genetic alterations in human leukemia. Although the mechanisms are likely to differ, all rearranged forms of MLL positively upregulate expression of *HOX* genes including *HOXA9* and the HOX cofactor *MEIS1*, which has been shown to be critical for transformation (Armstrong et al., 2002; Ayton and Cleary, 2003; Kumar et al., 2004). The most common *MLL* rearrangements are balanced translocations that account for up to 80% of infant acute leukemia and approximately 5%–10% of adult acute myeloid leukemia (AML) and acute lymphoid leukemia (ALL) cases (Aplan, 2006; Hess, 2004). The resulting oncogenic fusion proteins fuse approximately 1400 N-terminal amino acids of MLL in frame to one of over 60 different translocation partners (Krivtsov and Armstrong, 2007). The breakpoint cluster region in MLL invariably includes the CxxC domain and adjacent RD2 region in MLL fusion proteins, but deletes the downstream PHD fingers and SET domain (Zhang and Rowley, 2006). Because the SET domain is lost during rearrangement, MLL fusion proteins activate transcription through mechanisms dependent on the translocation partner. The most common of these fusion proteins involve translocations between MLL and nuclear translocation partners including AF9, AF4, and ENL, among others, that interact with a complex of proteins termed ENL associated proteins (EAPs) or a closely related complex called AEP for AF4 family/ENL family/P-TEFb complex (Yokoyama et al., 2010). In addition to the most common MLL translocation partners, EAP includes

Significance

Translocations involving the *MLL* gene create potent oncogenic fusion proteins that account for up to 80% of infant acute leukemias, underscoring the importance of understanding the molecular mechanisms driving oncoprotein function. Using biochemical approaches we have identified direct physical interaction of the PAF complex (PAFc) with sequences invariably retained in MLL fusion proteins. At a molecular level we show PAFc is required for full MLL fusion protein mediated transcriptional activation and for proper recruitment of MLL to target genes. This study demonstrates that PAFc is an essential co-factor for MLL fusion proteins that is necessary in vivo for cell immortalization and consequently may serve as an attractive new therapeutic target for leukemias with *MLL* rearrangements.

the histone H3 lysine 79 methyltransferase hDOT1L and transcription elongation factors CDK9 and cyclinT1 (collectively known as pTEFb) (Krivtsov et al., 2008; Mueller et al., 2007).

Several structural domains have been identified in MLL and MLL fusion proteins that are required for transcriptional activity. Identifying these domains and their molecular interactions is important because of their promise for therapeutic targeting. For example, interaction of N-terminal sequences of MLL in a trimolecular complex with Menin and LEDGF is required for targeting the fusion protein to chromatin and for leukemogenicity (Caslini et al., 2007; Yokoyama and Cleary, 2008; Yokoyama et al., 2005). The DNA methyltransferase homology region or CxxC domain of MLL binds nonmethylated CpG islands and protects against DNA methylation (Ayton et al., 2004; Erfurth et al., 2008). Point mutations that block DNA binding by this region also block immortalization (Ayton et al., 2004).

In addition to the CxxC domain itself, regions immediately adjacent to the CxxC domain also appear to be important for MLL function. In the study by Bach et al. involving domain swaps between MLL1 and MLL2, the CxxC domain along with flanking sequences of MLL1 were essential for immortalization by MLL fusion proteins (Bach et al., 2009). In particular, immortalization was dependent on MLL sequences between amino acids (aa) 1149 and 1154 (the so-called pre-CxxC domain) as well as sequences in the adjacent basic ''post-CxxC'' or RD2 region between aa 1298 and 1337 (Ayton et al., 2004; Bach et al., 2009).

Increasing evidence shows that both histone H3 lysine 4 (H3K4) methylation, which is mediated by MLL, among other methyltransferases, and histone H3 lysine 79 (H3K79) methylation-mediated by DOT1L, which is recruited by MLL fusion proteins, is dependent on histone H2B monoubiquitination. The polymerase associated factor complex (PAFc) plays a critical role in mediating H2B ubiquitination as well as promoting H3K4 and H3K79 methylation (Dover et al., 2002; Krogan et al., 2003; Ng et al., 2003; Sun and Allis, 2002). PAFc is composed of five subunits in mammals including PAF1, LEO1, CDC73, CTR9, and WDR61 (Rozenblatt-Rosen et al., 2005; Zhu et al., 2005a).

The role of PAFc in transcriptional regulation is beginning to be better defined. PAFc was originally identified as a protein complex in yeast that associates with RNA polymerase II (RNAP II) (Wade et al., 1996). The complex associates with both initiating (Ser5-phosphorylated) and elongating (Ser2-phosphorylated) RNAPII (Pokholok et al., 2002). Increasing evidence suggests that in mammals many genes controlling development, including the *Hox* genes, are regulated at the level of transcriptional elongation (Chopra et al., 2009). At such ''pause prone'' promoters, RNA polymerase II (RNAPII) interacts with two complexes that inhibit transcriptional elongation, *n*egative *el*ongation *f*actor (NELF) and *D*RB *s*ensitivity-*i*nducing *f*actor (DSIF). NELF is a complex of four subunits that binds to the unphosphorylated RNAPII C-terminal domain (CTD) and induces proximal promoter pausing. DSIF is composed of a heterodimer of hSpt4 and hSpt5 that plays a dual role in both transcriptional activation and repression. hSpt5 contains six copies of the sequence G-S-R/Q-T-P (the C-terminal repeats or CTR), which is similar in sequence to the RNAPII CTD Y-S-P-T-S-P-S. When the CTR is unphosphorylated, DSIF represses transcriptional elongation. As an early step in transcriptional activation, pTEF-b phosphorylates both the Pol II CTD as well as the hSpt5 CTR. CTD phosphorylation releases NELF. Importantly phosphorylation of the hSpt5 CTR in DSIF also promotes recruitment of PAFc (Liu et al., 2009).

Once recruited, PAFc then has two critical activities. One is the recruitment of the E2 ubiquitin ligase RAD6 and the E3 ubiquitin ligase BRE1 (in mammals hBRE1A/RNF20 and BRE1B/RNF40), which is mediated through either a direct or indirect interaction between PAF1 and BRE1 (Kim et al., 2009; Pavri et al., 2006). Importantly, the interaction with PAF1 not only recruits BRE1 and RAD6 but also stimulates the ubiquitinating activity of the heterocomplex for histone H2B lysine 120. In yeast this is followed by recruitment of the proteosomal ATPases Rpt4 and Sug1 (Rpt6) and methylation by the yeast MLL complex homolog COMPASS, which is recruited by interaction with monoubiquitinated histone H2B via the Cps35 subunit as well as through PAF1 (Krogan et al., 2003; Lee et al., 2007). However, the human homolog of Cps35, WDR82, doesn't interact with MLL complexes (Wu et al., 2008), suggesting that MLL is recruited by alternative mechanisms.

In this study, we investigated the importance of PAFc in MLL transcriptional activation and MLL fusion protein transformation.

RESULTS

PAFc Interacts with the CxxC-RD2 Domain of MLL

In order to identify proteins that associate with MLL CxxC-RD2, we expressed epitope tagged portions of this region transiently in human embryonic kidney 293 cells (Figure 1A). Flag-tagged CxxC-RD2 including a nuclear localization signal (NLS) was immunoprecipitated from transiently transfected 293 cells using M2 anti-Flag agarose beads. An ''empty'' expression vector with Flag epitope tag and NLS was also subjected to immunoprecipitation as a nonspecific immunoprecipitation control. Coeluted proteins were resolved by SDS-PAGE (Figure 1B) and analyzed by mass spectroscopy. Multiple peptides corresponding to subunits of PAFc were identified with high probability including CTR9, LEO1, PAF1, CDC73, and WDR61 that correlated with silver stained bands at 133 kDa, 105 kDa, 75 kDa, 64 kDa, and 34 kDa, respectively (Figure 1B). Each of the five PAFc subunits identified by mass spectrometry (PAF1, CDC73, CTR9, LEO1, and WDR61) was confirmed to coimmunoprecipitate with Myc-tagged CxxC-RD2 by western blotting in 293 cells (Figure 1C). To exclude the possibility of a DNA-mediated MLL-PAFc interaction and confirm that the PAFc interaction is preserved in the context of a fusion protein, we repeated immunoprecipitations with Myc-tagged CxxC-RD2-AF9 in 293 cells after Benzonase treatment (see Figure S1A available online). Immunoprecipitation was preserved in the presence of Benzonase indicating the interaction is not DNA dependent (Figure 1D). Furthermore, PAFc coimmunoprecipitated with Myc-CxxC-RD2-AF9 (Figure 1D), as well as, Myc-CxxC-RD2 (Figure S1B). These experiments were repeated with transfection of an expression vector for Flag-tagged full-length MLL or Flag-tagged MLL-AF9 into 293 cells followed by immunoprecipitation and western blotting (Figures 1E and 1F). We also confirmed the PAFc interaction by coimmunoprecipitation of CDC73 with MLL-ENL in the KOPN8 cell line (Figure S1C). Together, these experiments show the MLL-PAFc interaction is maintained both in the context of full-length

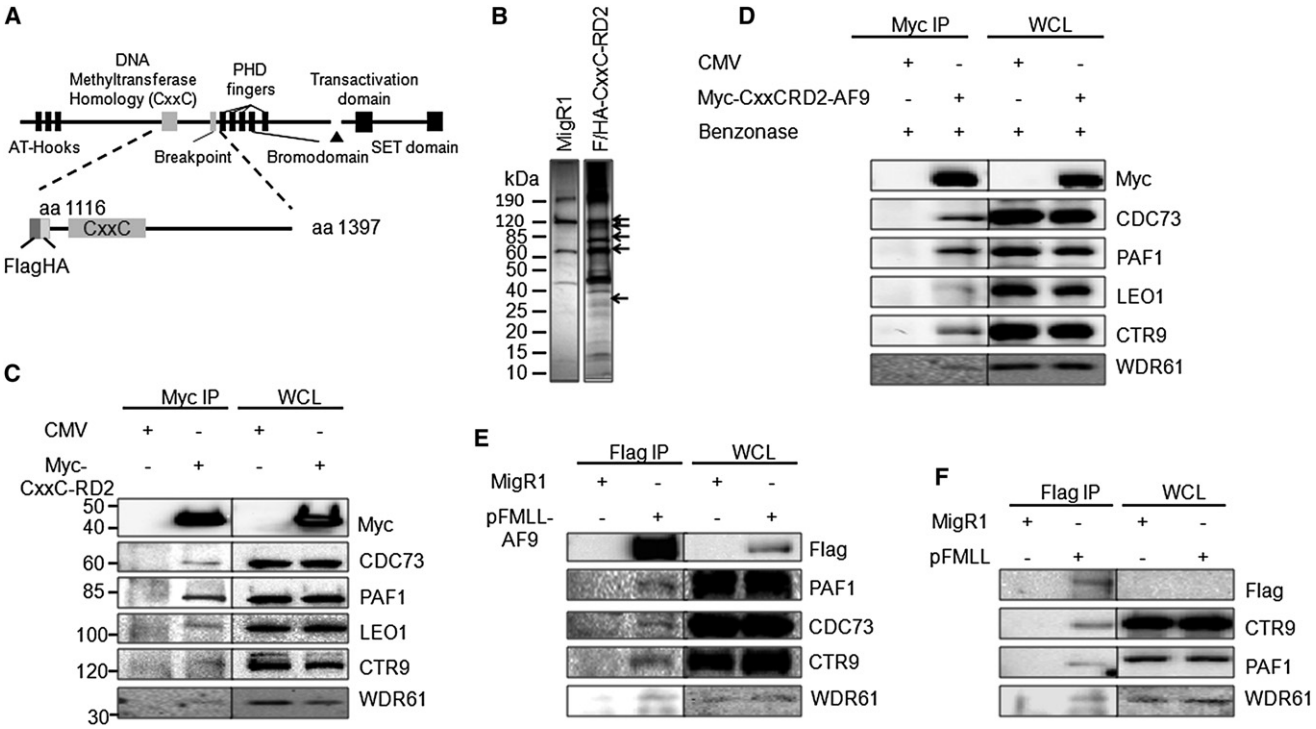

Figure 1. MLL Binds to the PAF Complex in a DNA-Independent Manner

(A) Schematic diagram of the full-length MLL protein with key domains indicated. The Flag/HA-tagged CxxC-RD2 MLL fragment used for immunoprecipitation is shown below. The first and last amino acids of the protein fragments are indicated.

(B) MigR1 and Flag/HA-tagged CxxC-RD2 was expressed in 293 cells and immunoprecipitated. Immunoprecipitates were analyzed by SDS-PAGE and visualized by silver staining. Arrows indicate bands at the predicted molecular weights of the PAF complex components.

(C) Immunoprecipitation and western blot of the PAF complex after immunoprecipitation of Myc-tagged CxxC-RD2 or Myc tag control from transiently tranfected 293 cells.

(D) The experiment described in (C) was repeated after treatment of the lysate with benzonase to digest DNA, indicating the PAFc interaction with CxxC-RD2 is DNA independent. Myc-tagged CxxC-RD2-AF9, but not the Myc tag alone, interacts with PAFc subunits, showing that PAFc binding to CxxC-RD2 is maintained in the presence of the AF9 translocation partner.

(E and F) A full-length Flag-tagged MLL-AF9 fusion protein (E) or Flag-tagged full-length MLL (F) was expressed in 293 cells and immunoprecipitated. The PAF complex stably associated with full-length MLL fusion protein and MLL as indicated by western blotting. See also Figure S1.

(MLL^N) as well as in the context of a leukemogenic MLL fusion protein (Figures 1E and 1F, Figure S1C).

To determine whether the interaction between MLL and PAFc is direct and to identify the PAFc subunit(s) involved, we bacterially expressed and purified the MLL CxxC-RD2 region (aa 1115–1396) and the RD2 region alone (aa 1202–1396) for in vitro pull-down experiments with bacterially expressed PAF1, LEO1, CDC73 and CTR9 (expressed as N- and C-terminus proteins termed CTR9-N and CTR9-C) (Figures 2A and 2B). These in vitro immunoprecipitations were performed with either CxxC-RD2 or RD2 with MLL antibodies after incubation with individual components of PAFc. Strong interaction of PAF1 with CxxC-RD2 but not the RD2 region was detected indicating an interaction between PAF1 and amino acids 1115 and 1201 of MLL (Figure 2C). These findings are consistent with our in vivo immunoprecipitation experiments in which PAFc co-immunoprecipitated with a small fragment of MLL N-terminal to the CxxC domain (amino acids 1115–1154) (Figure 3, see below). We also detected a second interaction between CTR9-C and both the MLL CxxC-RD2 and RD2 regions (Figure 2C). In addition a weak association of CDC73 with RD2 was also detected. These interactions were confirmed by reciprocal MBP pull down of CDC73, CTR9-N and CTR9-C, which showed that the MLL CxxC-RD2 and RD2 regions specifically associated with CTR9-C, along with a weak interaction detected between RD2 and CDC73 (Figure S2).

We then performed a series of deletion experiments to further map the MLL residues that participate in the MLL-PAFc interaction. Expression vectors for Myc-tagged CxxC-RD2-AF9 deletion mutants spanning the RD2 region of MLL (Figure 3A, Cx-1154-AF9 through Cx-1357-AF9) were transiently transfected into 293 cells and tested for PAFc interaction. These experiments reveal a sharp decrease in the MLL-PAFc interaction when C-terminal deletions were made past amino acid 1299 (Figure 3B, compare lanes 6 and 7). To overcome the residual low level binding of PAFc with proteins deleted at aa 1209 or aa 1258, believed to be the result of pre-CxxC interaction (Figure 2), we repeated this experiment with a set of deletion constructs that begin with MLL aa 1180 thereby deleting the proximal site of PAFc interaction (Figure 3C, Cx-del-1209-AF9 through Cx-del-1357-AF9). These experiments showed PAFc interaction with MLL is completely eliminated with deletions

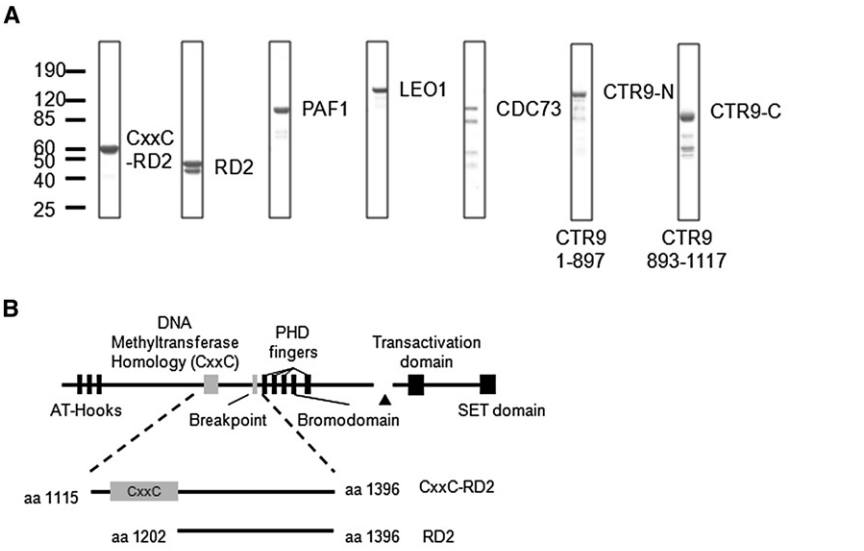

Figure 2. PAF1 and CTR9 Bind Directly to the CxxC-RD2 Region of MLL

(A) Coomassie blue staining of bacterially purified His-MOCR-tagged CxxC-RD2, RD2, PAF1, LEO1, and His-MBP-tagged CDC73, CTR9-N, and CTR9-C. The amino acids of CTR9-N and CTR9-C are indicated.

(B) Schematic diagram of MLL and bacterially purified CxxC-RD2 and RD2 regions. Starting and ending amino acids are indicated.

(C) Immunoprecipitations performed with bacterially purified recombinant CxxC-RD2 or RD2 and PAF complex components. Individual PAF components were incubated with either CxxC-RD2 or RD2 and immunoprecipitated with MLL antibodies. PAF components and immunoprecipitated MLL fragments were detected with the indicated antibodies by western blotting. Asterisk denotes detection of the IgG heavy chain. See also Figure S2.

beyond aa 1299 (Figure 3D, compare lanes 4 and 5). Together, our data suggest the MLL-PAFc interaction is multivalent involving residues of MLL both in the pre-CxxC domain as well as the RD2 region. Furthermore, the binding of PAFc by both pre- and post-CxxC domains is consistent with the solution structure of the MLL CxxC domain (Protein Data Bank [PDB] ID code 2J2S) (Allen et al., 2006), which shows the DNA binding CxxC domain coordinates two zinc atoms thereby bringing the pre- and post-CxxC regions into close opposition (Figure 8D).

PAFc Stimulates Transcriptional Activity by MLL and MLL Fusion Proteins

We then tested whether PAFc affects the transcriptional output mediated by MLL and the MLL-AF9 fusion protein. Dual luciferase assays were performed in 293 cells transfected with a luciferase reporter construct under the transcriptional control of the murine *Hoxa9* promoter (*Hoxa9-LUC*). These experiments showed that transcriptional activation by wild-type MLL is enhanced by coexpression of the five PAFc subunits (Figure 4A). Consistent with our earlier finding (Milne et al., 2002), we observed a dose-dependent transcriptional activation of the *Hoxa9* promoter by expression of increasing amounts of MLL-AF9 (Figure 4B). Furthermore, we observed a dose-dependent augmentation of MLL-AF9 dependent transcription of the *Hoxa9* promoter when increasing amounts of PAFc were expressed. Notably, expression of PAFc alone had little effect on the *Hoxa9* promoter in our assay (Figures 4A and 4B). A similar trend was observed when using an MLL-AF9 responsive luciferase construct containing a *thymidine kinase* promoter and multimerized *Myc E-boxes* (Figures S3A and S3B). Furthermore, we did not observe augmented transcription when single PAF components were introduced (Figure 4C). Deletion of the RD2 region to amino acid 1258 (which abrogates PAFc binding [Figure 3]) in an MLL-AF9 fusion protein also diminishes transcriptional activation (Figure S3C, compare lanes 5 and 6). Deletion of RD2 past aa1299 diminishes transactivation despite the more proximal PAFc interaction site and CxxC domain remaining intact, demonstrating the importance of the multivalent interaction for transcription. Together, these findings show MLL and MLL-AF9 synergize with PAFc to augment transcription of target genes.

MLL Fusion Protein-Mediated Transformation Is Dependent upon Interaction with PAFc

We then tested whether the transforming potential of MLL fusion proteins is dependent on the MLL-PAFc interaction. The deletions in the MLL RD2 region tested in immunoprecipitations described above (Figure 3A) or the pre-CxxC region were cloned into full-length MLL-AF9 in MSCV-based retroviral vectors (Figure 5D). These were packaged in Plat-E cells and transduced into 5-FU primed bone marrow and analyzed in methylcellulose replating assays as previously described (Morita et al., 2000). In brief, transduced cells were cultured under G418 selection in the presence of IL3, IL6, GM-CSF, and SCF and colonies quantitated after the first, second and third rounds of replating (Figure 5A). Western blotting confirmed proteins of the predicted molecular weights were expressed following transient transfection of Plat-E cells (Figure 5C). In addition, real-time polymerase chain reaction (PCR) confirmed expression of fusion gene mRNA in retrovirally transduced bone marrow (Figure 5B).

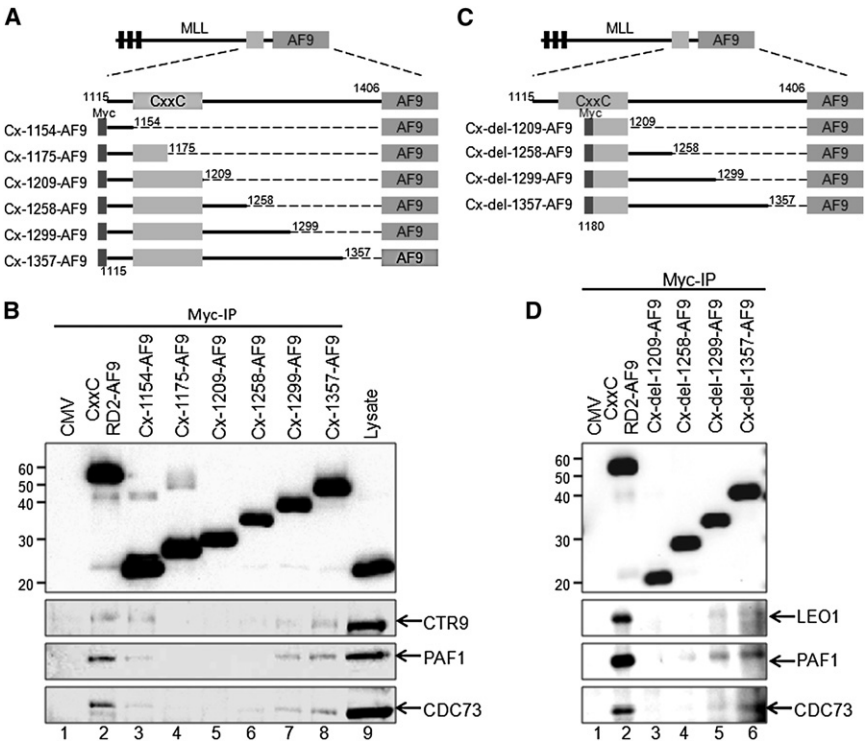

Figure 3. Amino Acids within the RD2 Region Are Necessary for MLL Interaction with the PAF Complex

(A) Schematic of Myc-tagged CxxC-RD2-AF9 constructs made with serial deletions of the RD2 region. The first and last MLL amino acid retained in the expression constructs are indicated. All constructs include the AF9 fusion partner at the C terminus and Myc tag at the N terminus. The Cx-1154-AF9 through Cx-1357-AF9 constructs are named according to the last MLL residue retained in the fusion protein.

(B) Myc-tagged RD2 deletion constructs described in (A) were expressed in 293 cells and then immunoprecipitated. The Myc-tagged MLL deletion proteins and associated PAF complex components were detected by western blotting with the indicated antibodies.

(C) Schematic of a second set of deletion constructs made through the RD2 region that also delete the pre-CxxC domain. Cx-del-1209-AF9 through Cx-del-1357-AF9 were made by deleting amino acids 1115 through 1179 of MLL. The amino acids included in each construct are indicated.

(D) Myc tagged constructs described in (C) were expressed in 293 cells, immunoprecipitated and detected as described in (B).

As shown in Figures 5D and 5G, similar numbers of tertiary colonies were observed when cells were transduced with MLL-AF9, MLL-1357-AF9, or MLL-1299-AF9. Further deletions of RD2 that extended more proximally than amino acid 1299, which markedly reduced PAFc interaction in our immunoprecipitation experiments (Figure 3), resulted in marked decreases in colony numbers (Figure 5D and 5G). Importantly, the morphology of these colonies was also dramatically different. Tertiary colonies from MLL-AF9, MLL-1357-AF9, and MLL-1299-AF9 all displayed a dense, compact morphology indicative of transformation (Lavau et al., 1997) (Figure 5E). Wright Giemsa-stained cytospins showed these compact colonies were composed of

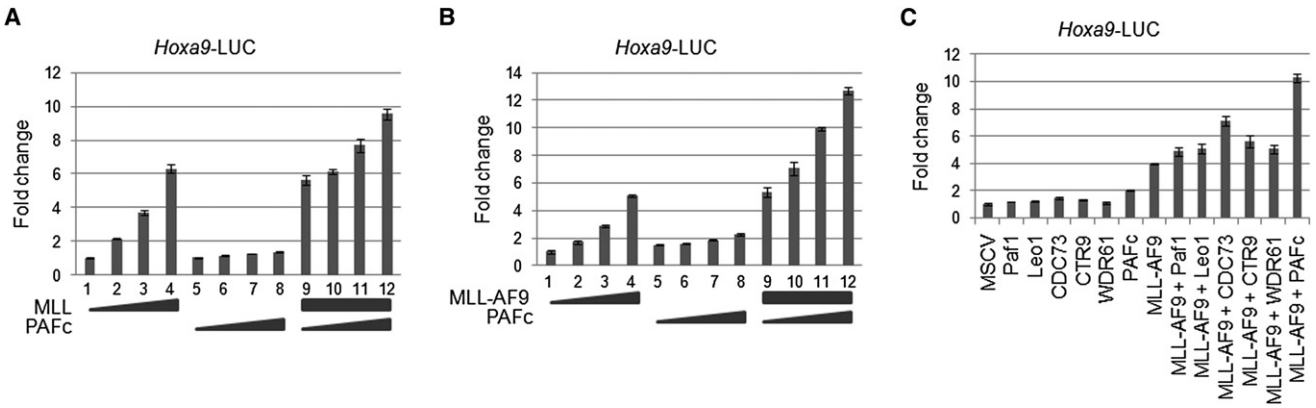

Figure 4. The PAF Complex Synergizes with MLL and MLL-AF9 to Augment Transcriptional Activity

(A) Luciferase assays were performed with the *Hoxa9-LUC* reporter construct and increasing doses of full-length MLL (lanes 1–4) (0 –0.6 μg) or PAFc (lanes 5–8) (0–0.6 μg). PAFc includes equal amounts of PAF1, LEO1, CDC73, CTR9, and WDR61. Lanes 9–12 show constant MLL (0.6 μg) with increasing doses of PAFc (0–0.6 μg). All changes are shown relative to lane 1, which includes *Hoxa9-LUC* and an empty expression vector. Error bars indicate standard deviation (SD). Results of one of more than three representative experiments performed are shown.

(B) Experiment was performed as described in (A) except increasing doses of MLL-AF9 (0–0.6 μg) were used in lanes 1–4. Lanes 5–8 show increasing doses of PAFc (0–0.6 μg). Lanes 9–12 show increasing doses of PAFc (0–0.6 μg) in the presence of constant MLL-AF9 (0.6 μg). Error bars indicate ± SD. One of three representative experiments is shown.

(C) Luciferase assay performed in transfected 293 cells with the *Hoxa9-LUC* reporter construct and individual PAFc components in lanes 1–6, the PAF complex (lane 7), MLL-AF9 alone (lane 8), MLL-AF9 plus individual PAF components (lanes 9–13), and MLL-AF9 with the PAF complex (lane 14). Error bars indicate ± SD. Results of one of more than three representative experiments are shown. See also Figure S3.

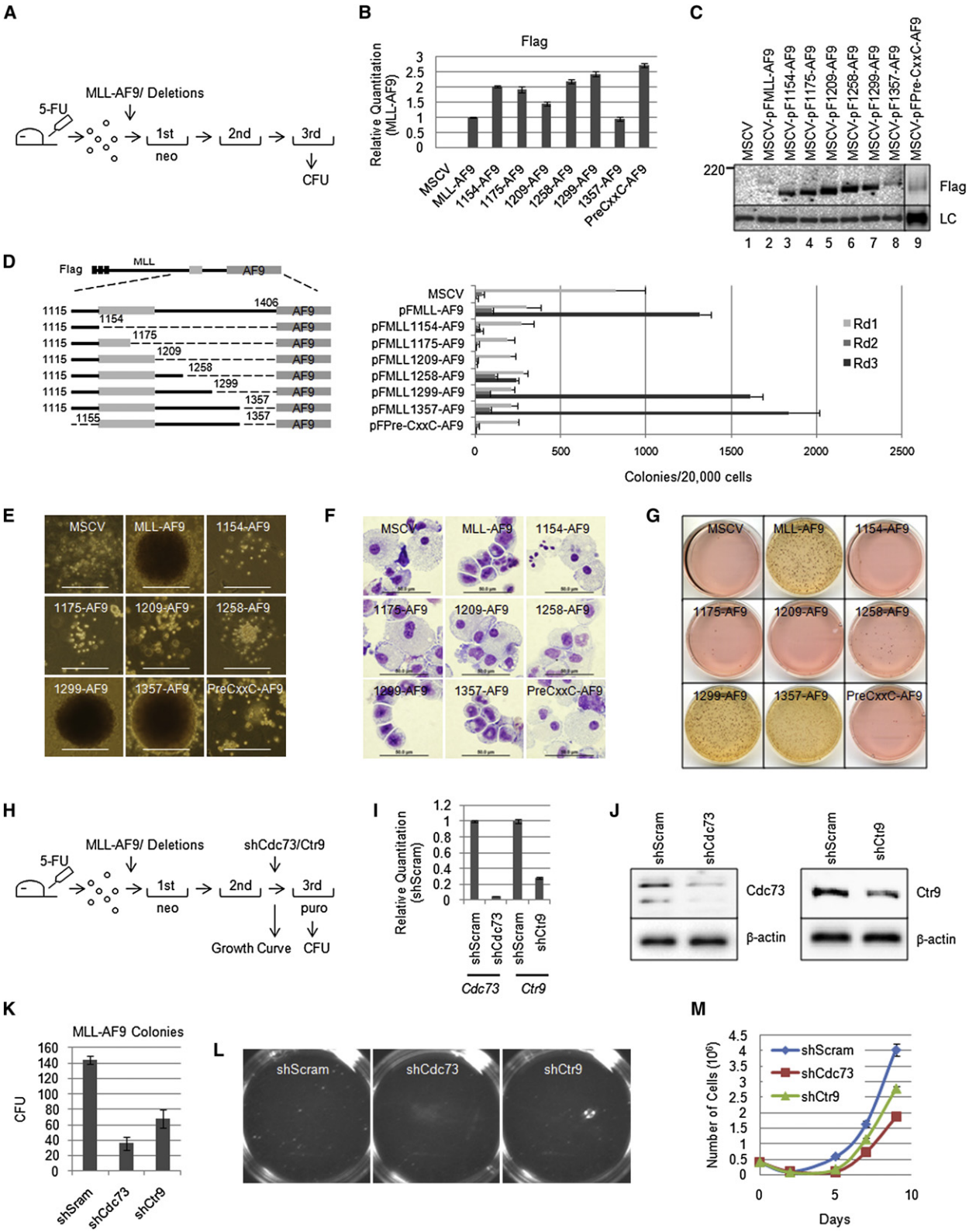

Figure 5. The PAFc Interaction Surface on RD2 Is Necessary for Bone Marrow Transformation by MLL-AF9 Fusion Proteins

(A) Schematic diagram for MLL-AF9 and MLL-AF9 deletion colony forming assay.

(B) Real-time qPCR using primers for the Flag tag on the MLL-AF9 fusion proteins. qPCR was performed on cDNA from bone marrow cells after retroviral transduction. Expression levels are shown relative to MLL-AF9 transduced cells. Error bars indicate ± SD.

myeloblasts (Figure 5F). In contrast, transductions of constructs with more extensive deletions resulted in diffuse colonies composed of differentiating myeloid cells including monocytes and macrophages (Figures 5E–5G). Of note, MLL-1258-AF9 retained a limited capacity to produce dense colonies after tertiary replating, but colony numbers were significantly reduced compared to MLL-AF9, MLL-1357-AF9, and MLL-1299-AF9 (Figures 5D, 5E, and 5G). In keeping with this, minimal binding of PAFc was observed with the Cx-1258-AF9 construct (Figure 3). As expected, MLL-AF9, as well as, 1357 and 1299 deletions markedly upregulated *Hoxa9* expression, while forms incapable of PAFc interaction did not (Figure S4B). The loss of MLL fusion protein mediated transformation upon deletion of the pre-CxxC and RD2 domains is comparable to the result of deleting the DNA binding CxxC domain (MLL-1154-AF9), which has been previously shown to be required for transformation (Ayton et al., 2004; Bach et al., 2009). To eliminate the possibility that the deletions introduced prevent interaction with the enzymatic activities necessary for leukemogenesis, we performed immunoprecipitations with the RD2 deletions constructs described in Figure 3. These experiments showed that association of DOT1L and the pTEFb component, cyclin T1, with AF9 is maintained in all the deletion constructs used (Figure S4A). This suggests improper transformation activity is due solely to functions dependent on the RD2 region and not misfolding of proteins or deficient EAP complex recruitment (Figure S4A). To confirm PAFc is necessary for MLL-AF9-mediated transformation, we performed colony assays by transducing bone marrow cells with MLL-AF9 followed by a second round of transduction with shRNA retroviruses directed against Cdc73 or Ctr9 (Figure 5H). Both shCdc73 and shCtr9 were confirmed to knock down Cdc73 and Ctr9, respectively, at the mRNA and protein level (Figures 5I and 5J). Knockdown of either Cdc73 or Ctr9 resulted in significantly reduced colony formation compared with a scrambled control shRNA (Figures 5K and 5L). These data were confirmed with an established MLL-AF9 cell line (Figures S4C and S4D). We also observed a significantly reduced proliferation rate when either Cdc73 or Ctr9 was knocked down in primary cells grown in liquid culture in the presence of IL3 and SCF (Figure 5M). Reduced proliferation was also observed when Cdc73 or Ctr9 was knocked down in the MLL-AF9 cell line (Figure S4E). Together, these data suggest the PAFc interaction with MLL is crucially important for both MLL fusion protein mediated *Hox* deregulation and transformation.

PAFc Promotes MLL and MLL Fusion Protein Recruitment to Target Loci

We then examined the localization of PAFc to a leukemogenic target gene of MLL such as *Hoxa9*. For these experiments, we generated cell lines by transducing mouse bone marrow with either MLL-ENL or E2A-HLF. MLL-ENL cells express much higher levels of both *Hoxa9* and *Meis1* compared with E2A-HLF cells, which are not dependent on *Hoxa9* expression for transformation (Ayton and Cleary, 2003) (Figure 6A). We performed chromatin immunoprecipitation (ChIP) experiments for PAF components, PAF1, LEO1, CDC73, and CTR9 at the *Hoxa9* locus in both cell lines (Figure 6B). These experiments showed robust binding of MLL-ENL as detected by the ENL antibody in MLL-ENL cells compared with E2A-HLF cells (Figure 6B). Furthermore, levels of histone H3K79 di- and trimethylation are markedly elevated in MLL-ENL cells consistent with ENL mediated recruitment of DOT1L (Mueller et al., 2007). Importantly, the pattern of binding of PAFc components and MLL-ENL across the locus is similar, consistent with an MLL-PAFc interaction (Figure 6B). Sequences downstream of the *Hoxa9* locus also show a dramatic decrease in binding of both MLL-ENL and PAFc (Figure S5). MLL-ENL binding is somewhat more abundant upstream and downstream of the transcriptional start site which may reflect a PAFc independent function for MLL fusion proteins during transcriptional elongation (Figure 6B). Similarly, we also observed co-localization of MLL-ENL and PAFc at the *Meis1* locus in MLL-ENL cells, with minimal binding seen in E2A-HLF cells (Figure 6C). Together, these data suggest that PAFc localizes with MLL fusion proteins to augment *Hox* and *Meis1* transcription.

To further evaluate the role of PAFc in transcriptional activation, we measured the effect of PAFc subunit knockdown on MLL-AF9 mediated transcriptional activation. Knockdown of

(C) Western blot for the MSCV-based Flag tagged MLL-AF9 deletion constructs shown in (D). Protein was extracted from transfected Plat-E cells and immunoprecipitated with M2 agarose beads. Proteins were detected with Flag antibodies. The loading control (LC) shows equal loading of protein.
(D) The constructs used for the retroviral infection and bone marrow colony assay are shown on the left. Final amino acids of the MLL deletions are shown. Primary, secondary, and tertiary colony counts are shown for methylcellulose colony assays performed with the indicated MLL-AF9 fusion proteins. Error bars indicate SD from duplicate experiments. One of more than three representative experiments is shown.
(E) Representative colony morphology is shown for each transduced MLL-AF9 fusion protein. Dense colonies are indicative of transformation while diffuse colonies indicate differentiation. Scale bars represent 500 μm.
(F) Wright-Giemsa-stained cytospins on cells isolated after the third round of methylcellulose plating. Scale bars represent 50 μm.
(G) Shown are p-iodonitro tetrazolium violet (INT)-stained colonies after three rounds of colony assay replating. Dense red colonies are visible from MLL-AF9, MLL-1299-AF9, and MLL-1357-AF9 transduced bone marrow.
(H) Schematic diagram for MLL-AF9 colony assay with shRNA mediated knockdown of Cdc73 and Ctr9. Colony assays were performed as described in (A) except for an additional transduction after the second replating with shScram, shCdc73, and shCtr9 retroviruses followed by plating in methylcellulose with puromycin selection. Colonies were scored after the third plating.
(I) Real-time qPCR was used to confirm knockdown of *Cdc73* and *Ctr9* mRNA compared with shScram after transduction of 3T3 cells. Error bars indicate ± SD.
(J) Protein lysate was collected from 3T3 cells transduced with shScram, shCdc73, and shCtr9 and separated by SDS-PAGE. Immunoblotting with Cdc73 and Ctr9 confirms knockdown of the respective proteins. β-actin was probed as a loading control.
(K) Third round colony counts after transduction with shScram, shCdc73, or shCtr9. Error bars indicate ± SD.
(L) Dense colonies are visible from colony assay plates containing shScram transduced cells. Significantly reduced colony numbers were visible from the shCdc73 and shCtr9 transduced cells.
(M) Cells collected after the second transduction with shRNA were grown in liquid culture in the presence of IL3, SCF, and puromycin. A significant proliferative advantage was observed from MLL-AF9 cells transduced with shScram compared with shCdc73 or shCtr9. Error bars indicate ± SD. See also Figure S4.

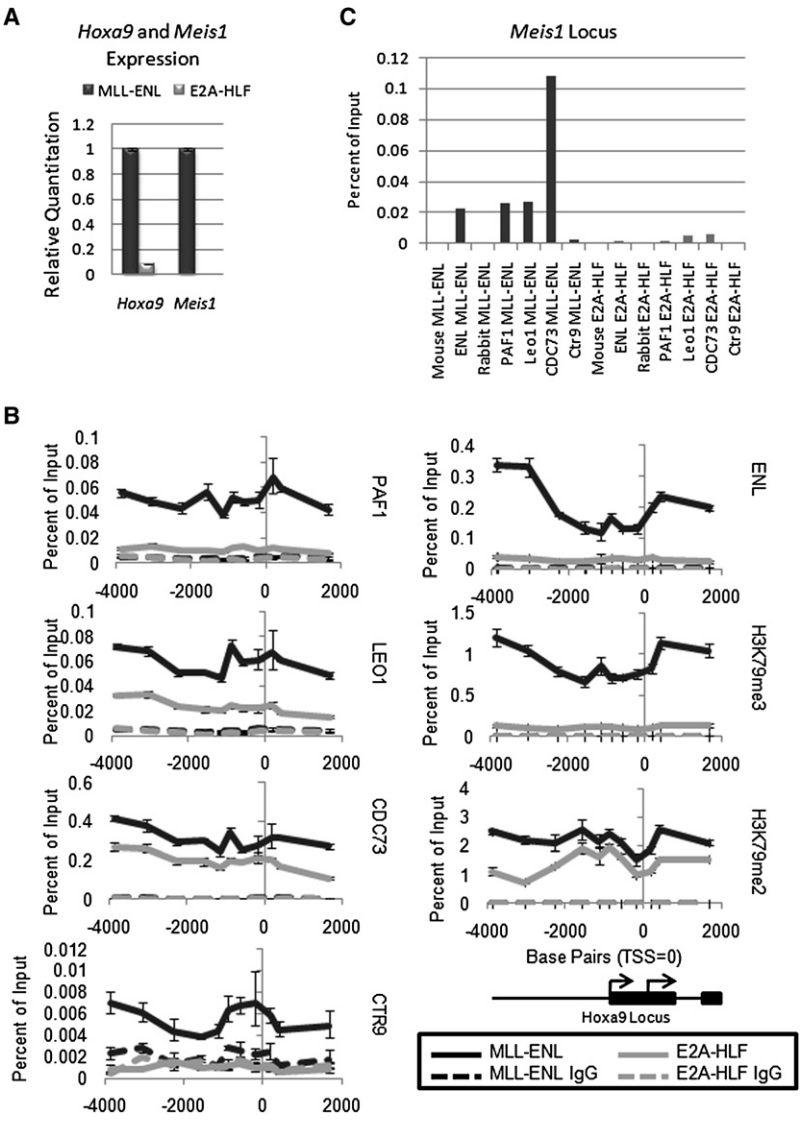

Figure 6. The PAF Complex Colocalizes with MLL-ENL across the *Hoxa9* Locus

(A) qPCR for *Hoxa9* and *Meis1* expression in MLL-ENL and E2A-HLF cell lines. Error bars indicate ± SD.

(B) ChIP experiment performed in mouse bone marrow cell lines established with the MLL-ENL or E2A-HLF fusion protein. MLL-ENL IPs are shown in black and E2A-HLF IPs are shown in gray. Solid lines indicate the binding pattern of the component or histone modification listed to the right. The dotted lines indicate control IgG IPs for each cell line. The *Hoxa9* locus is shown schematically at the bottom. Error bars indicate ± SD.

(C) Same experiment as described in (B), but binding was determined on the *Meis1* locus. The MLL-ENL IPs are shown in black (left) and the E2A-HLF IPs are shown in gray (right). See also Figure S5.

PAF1, LEO1, CDC73, and CTR9 was successfully achieved in HeLa cells with siRNA transfection (Figure 7A). As previously reported, PAFc knockdown decreases *HOXA9* expression in HeLa cells (Figure 7A) (Zhu et al., 2005b). Importantly, MLL-AF9 transcriptional activation of *Hoxa9-LUC* is also impaired by PAF1, LEO1, CDC73, or CTR9 knockdown (Figure 7B). Furthermore, we saw an additive effect by knocking down both CTR9 and LEO1, suggesting MLL fusion proteins require PAFc for efficient transcription of target genes (Figure 7B).

We then determined the effect of knockdown of the PAF complex on MLL recruitment to the *HOXA9* locus by performing ChIP assays on HeLa cells after simultaneous knockdown of CTR9, PAF1, CDC73, and LEO1 (Figure 7C). We observed a significant decrease in binding of CDC73, PAF1, and LEO1 in both the promoter and coding region of the *HOXA9* locus following knockdown, as expected, whereas histone H3 levels remain unchanged or elevated in siPAFc-treated cells (Figure 7D). PAFc knockdown resulted in a marked decrease in wild-type MLL binding compared with mock treated cells (Figure 7D), without affecting MLL protein levels (Figure 7C), suggesting PAFc is necessary for MLL recruitment to *HOXA9*. Consistent with reduced binding of MLL, knockdown of the PAF complex also resulted in a decrease in H3K4 tri-methylation at the *HOXA9* locus (Figure 7D). We also observed a decrease in histone H3K79 trimethylation (Figure 7D).

PAFc Expression Is Coordinately Downregulated during Myeloid Differentiation

The above results suggest that the PAF complex recruits MLL to the *HOXA9* locus and that modulating PAFc levels may be an important mechanism for modulating MLL activity. It is noteworthy in this regard that a recent unbiased genome-wide siRNA screen identified PAFc subunits Ctr9, Wdr61, and Rtf1 among the 30 top genes regulating Oct4 expression and stem cell renewal (Ding et al., 2009). In this study PAFc was found to bind to key pluripotency genes, which is remarkable because MLL fusion protein transformed cells show, in addition to *HOX* gene overexpression, a distinctive embryonic stem cell (ESC)-like pluripotency signature (Somervaille et al., 2009). Furthermore, expression of PAFc subunits is strongly regulated upon differentiation of ESCs into embryoid bodies (Ding et al., 2009). Collectively, these findings suggested that PAFc maintains pluripotency in hematopoietic progenitors.

We established two differentiation models to explore the potential role of PAFc in regulation during hematopoietic differentiation. First, we created a conditional AML cell line by immortalizing murine bone marrow by transduction with Hoxa9-ER in the presence of tamoxifen (4-OHT). Upon 4-OHT withdrawal, these cells undergo differentiation and cell-cycle arrest, which is largely complete by 120 hr (Figures S6A and S6B). 4-OHT withdrawal is accompanied by marked upregulation of *c-Fos* and *c-Jun* transcripts indicative of myeloid differentiation (Figure S6C). Microarray expression profiling was performed in triplicate at 24, 48, 72, 96, and 120 hr after 4-OHT withdrawal (only results for 72, 96, and 120 hr are shown in Figure 8A). These

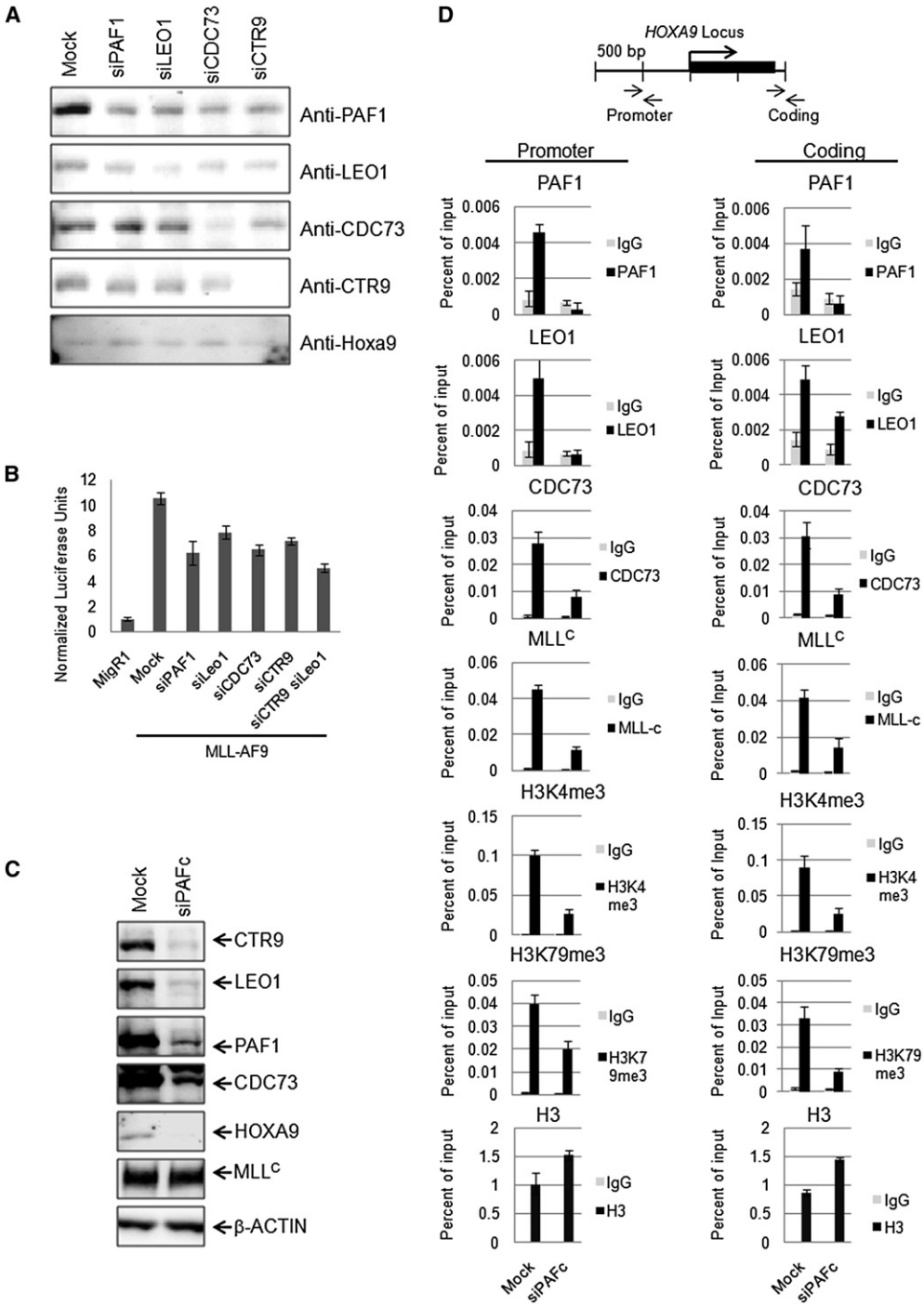

Figure 7. Knockdown of PAFc Reduces MLL-AF9-Mediated Transactivation and MLL Binding to the *HOXA9* Locus

(A) siRNA-mediated knockdown of individual PAF components was verified by western blotting. Antibodies used for western blotting are shown on the right and siRNA is indicated on top.

(B) Luciferase assays were performed with the *Hoxa9-LUC* reporter construct and MLL-AF9 in HeLa cells after transfection with the indicated siRNA. Luciferase units are shown relative to the MigR1 control transfected cells. Error bars indicate ± SD.

(C) Simultaneous siRNA mediated knockdown of PAFc (siCTR9, siLEO1, siPAF1, and siCDC73) is shown by western blotting for PAF components after siRNA transfection of HeLa cells. β-ACTIN was detected as a loading control.

(D) ChIP experiments were performed in HeLa cells after simultaneous knockdown of the PAF components shown in (C). PAF1, LEO1, CDC73, MLL^C, H3K4me3, H3K79me3, and H3 were immunoprecipitated from HeLa cells treated with siPAFc or nontargeting siRNA (Mock). Binding was assessed in both the promoter and coding region as indicated. A schematic of the *HOXA9* locus and location of the primer-probe sets used for qPCR are shown. Error bars indicate ± SD. One of more than three representative experiments is shown.

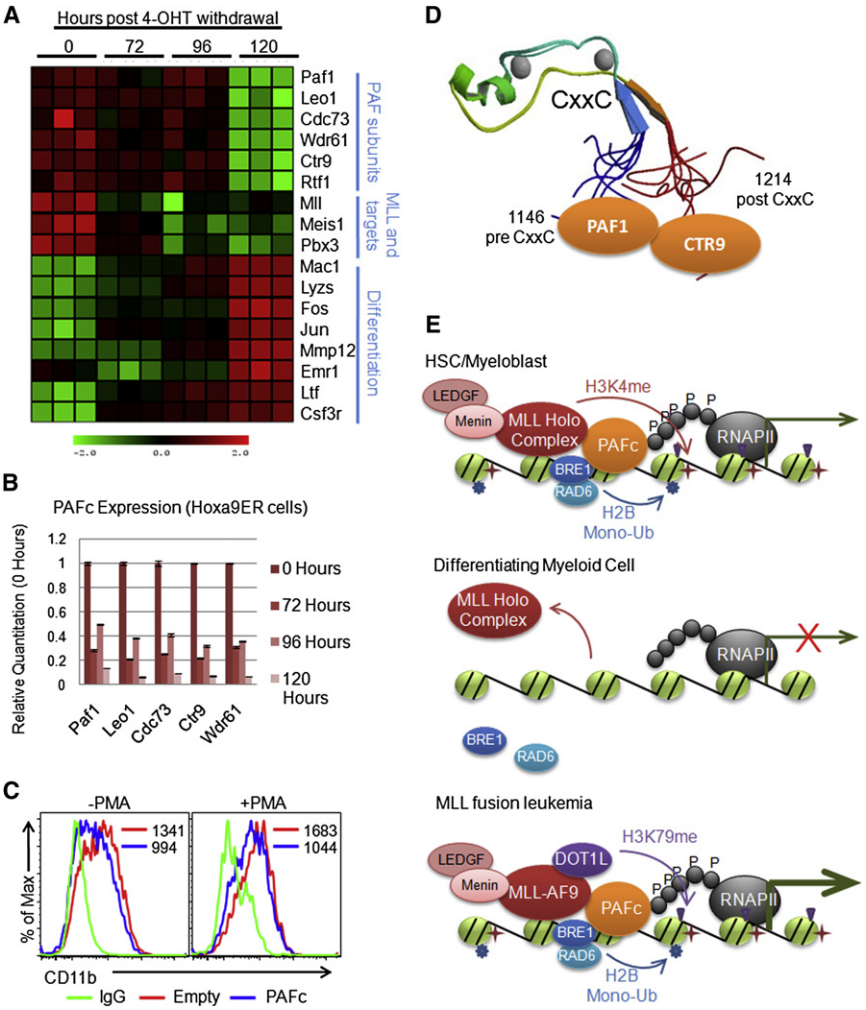

Figure 8. PAFc Is Downregulated during Differentiation of Hematopoietic Cells

(A) Heat map generated from expression array data collected from differentiation of the Hoxa9ER cell line. Data are shown in triplicate for each time point after tamoxifen withdrawal. Labels indicate components of the PAF complex, MLL, and MLL targets, and genes associated with myeloid cell differentiation.

(B) Expression of PAF components were verified using qPCR by separately differentiating the Hoxa9ER cell line by tamoxifen withdrawal. Time points indicate hours post tamoxifen withdrawal that RNA was collected. Expression for each component is shown relative to 0 hr. Error bars indicate ± SD.

(C) THP-1 cells were transfected with an equal mixture of PAFc expression vectors or empty vectors along with a GFP vector at a 5:1 ratio (PAFc/Empty:GFP). Half were treated with PMA to induce differentiation. Surface expression of CD11b was monitored by FACS in the GFP-positive gated cell population to track differentiation. Mean fluorescence values are shown for each sample.

(D) Structure of the CxxC domain and flanking sequences (PDB code: 2JYI). Solution structure of MLL CxxC region shows the flanking sequences of the CxxC domain brought into close juxtaposition creating a binding surface for both PAF1 and CTR9 of the PAF complex.

(E) Model for myeloid cell differentiation showing (top) PAFc dependent recruitment of MLL to target genes in hematopoietic progenitors (HSC/myeloblasts). PAFc and MLL recruitment promotes H2B monoubiquitination and H3K4 and H3K79 methylation resulting in transcriptional activation. In the middle image, more differentiated myeloid cells downregulate PAFc expression resulting in decreased recruitment and transactivation by MLL. As shown in the bottom image, in leukemic cells harboring MLL fusion proteins, the fusion protein synergizes with PAFc resulting in robust transcriptional activation of target genes. This is associated with increased H2B monoubiquitination and histone H3K79 methylation by DOT1L recruited through the MLL fusion partner. See also Figure S6.

experiments showed a marked downregulation of all PAFc subunits and MLL target genes after induction of differentiation accompanied by upregulation of genes associated with myeloid differentiation (Figure 8A). The downregulation of PAFc expression was confirmed by quantitative PCR (qPCR) in independently differentiated Hoxa9-ER cells (Figure 8B). We also analyzed the human HL-60 cell line, which rapidly differentiate into macrophages after exposure to phorbol 12-myristate 13-acetate (PMA) (Figure S6D). PMA treatment also led to a dramatic downregulation of PAFc in HL-60 cells (Figure S6E). To test the role of PAFc in hematopoietic differentiation, we enforced expression of PAFc in THP-1 cells with or without PMA-induced differentiation. THP-1 cells were more resistant to differentiation, as determined by CD11b surface expression, when PAFc was overexpressed (Figure 8C). Importantly, green fluorescent protein (GFP)-negative cells showed no significant difference in CD11b expression (Figure S6F). Together, these data show PAFc expression is specifically downregulated during myeloid differentiation and that high-level PAFc expression inhibits differentiation. Thus, PAFc may play an important role in regulating MLL binding to target genes during differentiation.

DISCUSSION

The work presented here establishes PAFc as an important cofactor for both transcriptional regulation by MLL as well as for leukemogenesis mediated by MLL fusion proteins. Interestingly several PAFc components have been previously implicated in carcinogenesis. Most notably mutations in CDC73 (Parafibromin), encoded by *HRPT-2* (hereditary hyperparathyroidism type 2), are responsible for the familial hyperparathyroidism-jaw tumor (HPT-JT) syndrome (Szabo et al., 1995). HPT-JT is an autosomal dominant disorder associated with hyperparathyroidism (HPT) and a high incidence of parathyroid adenomas, hyperplasias, and carcinomas as well as renal abnormalities and uterine tumors (Newey et al., 2009). The mutations in *HRPT-2* are predicted to lead to loss of function due to premature termination. The chromosome 1q25-q31 region spanning

HRPT-2 frequently undergoes loss of heterozygosity in tumors arising in HPT-JT patients, suggesting that CDC73 functions as a tumor suppressor (Newey et al., 2009). Consistent with this role, overexpression of wild-type CDC73, but not a mutant form found in HPT, blocks cell proliferation and inhibits the cell-cycle regulator cyclin D1 (Woodard et al., 2005).

However, other studies have implicated overexpression of PAFc subunits in tumorigenesis. For example, CDC73 overexpression in 293FT and COS7 cells increases S-phase entry and promotes cellular proliferation. This induction of CDC73-mediated cell dependent proliferation requires the SV40 large T-antigen, which is directly bound by CDC73 (Iwata et al., 2007). In a study to identify genes involved in pancreatic tumor progression, PAF1 was found to be overexpressed as a result of a double minute amplification involving chromosome 19q13 (Batra et al., 1991). Furthermore, overexpression of PAF1 results in transformation of NIH 3T3 cells (Moniaux et al., 2006).

The dual roles of CDC73 as a tumor suppressor and an ''aider and abettor'' of an oncoprotein (see above) are shared with another MLL-interacting protein, Menin. Menin interacts with the N terminus of MLL and is required for transformation by MLL fusion proteins (Caslini et al., 2007; Yokoyama et al., 2005). However, MEN1 mutations, which lead to loss of function of the Menin protein, are found in a variety of endocrine tumors including parathyroid hyperplasias and adenomas, as well as pancreatic islet tumor cells establishing Menin as a tumor suppressor (Chandrasekharappa et al., 1997; Lemmens et al., 1997). The similarities in the diseases associated with Menin and PAF subunit mutations (parathyroid and pancreatic islet tumors) raise the possibility that the mechanisms of oncogenicity may also be similar, perhaps mediated through cyclin-dependent kinase deregulation as we have previously defined for Menin (Milne et al., 2005b). These results also suggest that MLL may play a broader role in tumorigenesis than previously expected. Additional experiments will be necessary to assess what role MLL plays in cancers associated with disruption or amplification of PAF components.

Recently, genome-wide siRNA screens identified components of the PAF complex as important in maintaining an embryonic stem cell identity. PAFc was found to bind and regulate several key pluripotency genes including Oct4 (Ding et al., 2009). Downregulation of PAFc caused embryonic stem cell differentiation suggesting its expression is required to maintain an ESC identity. Our experiments show a similar coordinate regulation of PAFc in hematopoietic cells, where PAF component expression is strongly downregulated during myeloid differentiation (Figure 8). Recent gene expression profiling experiments have shown that MLL fusion proteins enforce expression of an ESC gene expression signature including the expression of *Myb*, *Hmgb3*, and *Cbx5*, which is necessary for the maintenance of the leukemic stem cell phenotype (Somervaille et al., 2009). Our data suggest that PAFc promotes MLL or MLL fusion protein recruitment to target loci in addition to its known role as a platform for recruitment of RAD6/BRE1 required for histone H2B ubiquitination and downstream histone H3K4 and H3K79 methylation (Figures 4 and 7). In this way MLL may be properly targeted to gene promoters in primitive hematopoietic cells, such as myeloblasts, through interaction with PAFc. During differentiation, downregulation of PAFc may be a mechanism for attenuating MLL binding to target genes as well as decreasing the histone H2B ubiquitination that is required for histone H3K4 and H3K79 methylation (Figure 8E). PAFc expression is high in leukemic cells, allowing for synergistic activation of key ECS pluripotency genes that appear to underlie MLL-mediated oncogenesis. It remains to be seen if MLL plays a role in enforcing the ECS signature that has been described for other particularly aggressive solid tumors (Ben-Porath et al., 2008; Gentles et al., 2009).

Our study identified two interaction sites between MLL and PAFc. The first involves an interaction with the MLL pre-CxxC domain between residues 1115 and 1154 and the PAFc subunit PAF1. In addition, under our immunoprecipitation conditions we observed a second interaction with CTR9 that occurs through the RD2 region (Figures 2 and 3; Figure S2). These findings are interesting in light of structural studies showing the CxxC domain of MLL forms a loop that interacts with DNA (Allen et al., 2006), thereby bringing the pre-CxxC sequence and the RD2 region into close juxtaposition in three dimensional space and creating a single binding surface for PAF1 and CTR9 (Figure 8D). It is intriguing in this regard that the region of RD2 necessary for a stable PAFc interaction is invariably conserved in MLL translocations, which involve breakpoints no more proximal than exon 8.

Our transformation assays indicate that both the pre-CxxC and RD2 interaction domains of MLL are required for transformation. We hypothesize that although the interaction between MLL and PAFc can occur through single contact points, it is only fully stable when both sites are intact. Given the importance of each of these MLL-PAFc domains for transformation (Figure 5), small-molecule inhibitors blocking either interaction would be expected to block oncogenesis by MLL fusion proteins. Given the general dependence of *HOX* expression on MLL, it is likely that inhibitors of this interaction will be effective in other leukemias showing high-level *HOX* and *MEIS1* expression, either as a result of MLL amplification or conceivably through other pathways. The experiments presented here lay the groundwork for determining the structure of the MLL-PAFc-interacting domain and the ultimate development of effective therapy based on targeting this interaction.

EXPERIMENTAL PROCEDURES

Cell Culture

293 and HeLa cells were cultured in Dulbecco's modified Eagle's medium (DMEM) supplemented with 10% fetal bovine serum (FBS) and 1X non-essential amino acids. MLL-ENL and E2A-HLF cells were cultured in Iscove's modified Dulbecco's medium (IMDM) supplemented with 15% fetal calf serum (FBS) (Stem Cell Technologies). Hoxa9ER cells were cultured in IMDM supplemented with 15% FBS and 0.1% IL3. Plat-E cells were cultured in DMEM supplemented with 10% FBS. HL-60, THP-1, KOPN8, and K562 cells were cultured in RPMI-1640 medium supplemented with 10% FBS. Differentiation of HL-60 and THP-1 cells was induced by 10 nM PMA treatment.

Luciferase Assay

293 cells were transiently transfected with MSCV MLL-AF9 (and derivatives), CMV-Renilla, and Hoxa9-LUC (or Myc-E box-LUC) constructs using FuGene 6 (Roche) in accordance with the manufacturer's instructions. Cells were then serum starved in 0.5% FBS in OPTI-MEM media for 48 hr. Luciferase assays were performed using the Dual Luciferase assay kit (Promega) according to manufacturer's instructions. Emission was detected using a Monolight 3010 (BD Biosciences).

Chromatin Immunoprecipitation

ChIP was performed as described previously (Milne et al., 2005a) using primary antibodies specific for MLL^C (gift from Dr. Yali Dou), ENL (gift from Dr. Robert Slany), histone H3, H3K4 dimethylation, H3K4 trimethylation, and H3K79 trimethylation (Abcam) and Paf1, Leo1, Parafibromin, and Ctr9 (Bethyl Laboratories, as described above). Quantitative real-time PCR was performed on the precipitated DNAs with TaqMan fluorescent labeling with primers and qPCR probes described in Supplemental Experimental Procedures. Binding was quantitated as follows: $\Delta C_T = C_T(\text{input}) - C_T(\text{Chromatin IP})$, % total = $2^{\Delta CT}$.

siRNA Knockdown of PAFc

siRNA smart pools were obtained from Dharmacon for CTR9, CDC73, PAF1, and LEO1. siRNA transfection of HeLa cells was achieved with Lipofectamine 2000 (Invitrogen) according to manufacturer's instructions for analysis in luciferase assays. Oligofectamine (Invitrogen) was used in accordance with the manufacturer's instructions for siRNA transfection of HeLa cells and PAFc knockdown for ChIP assays.

ACCESSION NUMBERS

Microarray data have been deposited in the Gene Expression Omnibus (GEO) repository from the National Center for Biotechnology Information (NCBI) with accession code GSE21299.

SUPPLEMENTAL INFORMATION

Supplemental Information includes six figures and Supplemental Experimental Procedures and can be found with this article online at doi:10.1016/j.ccr.2010.04.012.

ACKNOWLEDGMENTS

A.G.M. is supported by a postdoctoral training grant from the National Institutes of Health (T32 HL07622). Y.H. is supported by a University of Michigan Computational Medicine and Biology Pilot Research Grant. J.L.H. is supported by the National Institutes of Health (CA92251) and by a SCOR grant from the Leukemia and Lymphoma Society. We thank Dr. David Allis for sharing data prior to publication.

Received: November 2, 2009
Revised: February 3, 2010
Accepted: April 15, 2010
Published online: June 10, 2010

REFERENCES

Allen, M.D., Grummitt, C.G., Hilcenko, C., Min, S.Y., Tonkin, L.M., Johnson, C.M., Freund, S.M., Bycroft, M., and Warren, A.J. (2006). Solution structure of the nonmethyl-CpG-binding CXXC domain of the leukaemia-associated MLL histone methyltransferase. EMBO J. *25*, 4503–4512.

Aplan, P.D. (2006). Chromosomal translocations involving the MLL gene: Molecular mechanisms. DNA Repair (Amst.) *5*, 1265–1272.

Armstrong, S.A., Staunton, J.E., Silverman, L.B., Pieters, R., den Boer, M.L., Minden, M.D., Sallan, S.E., Lander, E.S., Golub, T.R., and Korsmeyer, S.J. (2002). MLL translocations specify a distinct gene expression profile that distinguishes a unique leukemia. Nat. Genet. *30*, 41–47.

Ayton, P.M., Chen, E.H., and Cleary, M.L. (2004). Binding to nonmethylated CpG DNA is essential for target recognition, transactivation, and myeloid transformation by an MLL oncoprotein. Mol. Cell. Biol. *24*, 10470–10478.

Ayton, P.M., and Cleary, M.L. (2003). Transformation of myeloid progenitors by MLL oncoproteins is dependent on Hoxa7 and Hoxa9. Genes Dev. *17*, 2298–2307.

Bach, C., Mueller, D., Buhl, S., Garcia-Cuellar, M.P., and Slany, R.K. (2009). Alterations of the CxxC domain preclude oncogenic activation of mixed-lineage leukemia 2. Oncogene *28*, 815–823.

Batra, S.K., Metzgar, R.S., and Hollingsworth, M.A. (1991). Isolation and characterization of a complementary DNA (PD-1) differentially expressed by human pancreatic ductal cell tumors. Cell Growth Differ. *2*, 385–390.

Ben-Porath, I., Thomson, M.W., Carey, V.J., Ge, R., Bell, G.W., Regev, A., and Weinberg, R.A. (2008). An embryonic stem cell-like gene expression signature in poorly differentiated aggressive human tumors. Nat. Genet. *40*, 499–507.

Caslini, C., Yang, Z., El-Osta, M., Milne, T.A., Slany, R.K., and Hess, J.L. (2007). Interaction of MLL amino terminal sequences with menin is required for transformation. Cancer Res. *67*, 7275–7283.

Chandrasekharappa, S.C., Guru, S.C., Manickam, P., Olufemi, S.E., Collins, F.S., Emmert-Buck, M.R., Debelenko, L.V., Zhuang, Z., Lubensky, I.A., Liotta, L.A., et al. (1997). Positional cloning of the gene for multiple endocrine neoplasia-type 1. Science *276*, 404–407.

Chopra, V.S., Hong, J.W., and Levine, M. (2009). Regulation of Hox gene activity by transcriptional elongation in Drosophila. Curr. Biol. *19*, 688–693.

Ding, L., Paszkowski-Rogacz, M., Nitzsche, A., Slabicki, M.M., Heninger, A.K., de Vries, I., Kittler, R., Junqueira, M., Shevchenko, A., Schulz, H., et al. (2009). A genome-scale RNAi screen for Oct4 modulators defines a role of the Paf1 complex for embryonic stem cell identity. Cell Stem Cell *4*, 403–415.

Dover, J., Schneider, J., Tawiah-Boateng, M.A., Wood, A., Dean, K., Johnston, M., and Shilatifard, A. (2002). Methylation of histone H3 by COMPASS requires ubiquitination of histone H2B by Rad6. J. Biol. Chem. *277*, 28368–28371.

Erfurth, F.E., Popovic, R., Grembecka, J., Cierpicki, T., Theisler, C., Xia, Z.B., Stuart, T., Diaz, M.O., Bushweller, J.H., and Zeleznik-Le, N.J. (2008). MLL protects CpG clusters from methylation within the Hoxa9 gene, maintaining transcript expression. Proc. Natl. Acad. Sci. USA *105*, 7517–7522.

Gentles, A.J., Alizadeh, A.A., Lee, S.I., Myklebust, J.H., Shachaf, C.M., Shahbaba, B., Levy, R., Koller, D., and Plevritis, S.K. (2009). A pluripotency signature predicts histologic transformation and influences survival in follicular lymphoma patients. Blood *114*, 3158–3166.

Hess, J.L. (2004). MLL: A histone methyltransferase disrupted in leukemia. Trends Mol. Med. *10*, 500–507.

Iwata, T., Mizusawa, N., Taketani, Y., Itakura, M., and Yoshimoto, K. (2007). Parafibromin tumor suppressor enhances cell growth in the cells expressing SV40 large T antigen. Oncogene *26*, 6176–6183.

Jude, C.D., Climer, L., Xu, D., Artinger, E., Fisher, J.K., and Ernst, P. (2007). Unique and independent roles for MLL in adult hematopoietic stem cells and progenitors. Cell Stem Cell *1*, 324–337.

Kim, J., Guermah, M., McGinty, R.K., Lee, J.S., Tang, Z., Milne, T.A., Shilatifard, A., Muir, T.W., and Roeder, R.G. (2009). RAD6-Mediated transcription-coupled H2B ubiquitylation directly stimulates H3K4 methylation in human cells. Cell *137*, 459–471.

Krivtsov, A.V., and Armstrong, S.A. (2007). MLL translocations, histone modifications and leukaemia stem-cell development. Nat. Rev. *7*, 823–833.

Krivtsov, A.V., Feng, Z., Lemieux, M.E., Faber, J., Vempati, S., Sinha, A.U., Xia, X., Jesneck, J., Bracken, A.P., Silverman, L.B., et al. (2008). H3K79 methylation profiles define murine and human MLL-AF4 leukemias. Cancer Cell *14*, 355–368.

Krogan, N.J., Dover, J., Wood, A., Schneider, J., Heidt, J., Boateng, M.A., Dean, K., Ryan, O.W., Golshani, A., Johnston, M., et al. (2003). The Paf1 complex is required for histone H3 methylation by COMPASS and Dot1p: linking transcriptional elongation to histone methylation. Mol. Cell *11*, 721–729.

Kumar, A.R., Hudson, W.A., Chen, W., Nishiuchi, R., Yao, Q., and Kersey, J.H. (2004). Hoxa9 influences the phenotype but not the incidence of Mll-AF9 fusion gene leukemia. Blood *103*, 1823–1828.

Lavau, C., Szilvassy, S.J., Slany, R., and Cleary, M.L. (1997). Immortalization and leukemic transformation of a myelomonocytic precursor by retrovirally transduced HRX-ENL. EMBO J. *16*, 4226–4237.

Lee, J.S., Shukla, A., Schneider, J., Swanson, S.K., Washburn, M.P., Florens, L., Bhaumik, S.R., and Shilatifard, A. (2007). Histone crosstalk between H2B monoubiquitination and H3 methylation mediated by COMPASS. Cell *131*, 1084–1096.

Lemmens, I., Van de Ven, W.J., Kas, K., Zhang, C.X., Giraud, S., Wautot, V., Buisson, N., De Witte, K., Salandre, J., Lenoir, G., et al. (1997). Identification

of the multiple endocrine neoplasia type 1 (MEN1) gene. The European Consortium on MEN1. Hum. Mol. Genet. *6*, 1177–1183.

Liu, Y., Warfield, L., Zhang, C., Luo, J., Allen, J., Lang, W.H., Ranish, J., Shokat, K.M., and Hahn, S. (2009). Phosphorylation of the transcription elongation factor Spt5 by yeast Bur1 kinase stimulates recruitment of the PAF complex. Mol. Cell. Biol. *29*, 4852–4863.

McMahon, K.A., Hiew, S.Y., Hadjur, S., Veiga-Fernandes, H., Menzel, U., Price, A.J., Kioussis, D., Williams, O., and Brady, H.J. (2007). Mll has a critical role in fetal and adult hematopoietic stem cell self-renewal. Cell Stem Cell *1*, 338–345.

Milne, T.A., Briggs, S.D., Brock, H.W., Martin, M.E., Gibbs, D., Allis, C.D., and Hess, J.L. (2002). MLL targets SET domain methyltransferase activity to Hox gene promoters. Mol. Cell *10*, 1107–1117.

Milne, T.A., Dou, Y., Martin, M.E., Brock, H.W., Roeder, R.G., and Hess, J.L. (2005a). MLL associates specifically with a subset of transcriptionally active target genes. Proc. Natl. Acad. Sci. USA *102*, 14765–14770.

Milne, T.A., Hughes, C.M., Lloyd, R., Yang, Z., Rozenblatt-Rosen, O., Dou, Y., Schnepp, R.W., Krankel, C., Livolsi, V.A., Gibbs, D., et al. (2005b). Menin and MLL cooperatively regulate expression of cyclin-dependent kinase inhibitors. Proc. Natl. Acad. Sci. USA *102*, 749–754.

Moniaux, N., Nemos, C., Schmied, B.M., Chauhan, S.C., Deb, S., Morikane, K., Choudhury, A., Vanlith, M., Sutherlin, M., Sikela, J.M., et al. (2006). The human homologue of the RNA polymerase II-associated factor 1 (hPaf1), localized on the 19q13 amplicon, is associated with tumorigenesis. Oncogene *25*, 3247–3257.

Morita, S., Kojima, T., and Kitamura, T. (2000). Plat-E: An efficient and stable system for transient packaging of retroviruses. Gene Ther. *7*, 1063–1066.

Mueller, D., Bach, C., Zeisig, D., Garcia-Cuellar, M.P., Monroe, S., Sreekumar, A., Zhou, R., Nesvizhskii, A., Chinnaiyan, A., Hess, J.L., and Slany, R.K. (2007). A role for the MLL fusion partner ENL in transcriptional elongation and chromatin modification. Blood *110*, 4445–4454.

Nakamura, T., Mori, T., Tada, S., Krajewski, W., Rozovskaia, T., Wassell, R., Dubois, G., Mazo, A., Croce, C.M., and Canaani, E. (2002). ALL-1 is a histone methyltransferase that assembles a supercomplex of proteins involved in transcriptional regulation. Mol. Cell *10*, 1119–1128.

Newey, P.J., Bowl, M.R., and Thakker, R.V. (2009). Parafibromin–functional insights. J. Intern. Med. *266*, 84–98.

Ng, H.H., Dole, S., and Struhl, K. (2003). The Rtf1 component of the Paf1 transcriptional elongation complex is required for ubiquitination of histone H2B. J. Biol. Chem. *278*, 33625–33628.

Pavri, R., Zhu, B., Li, G., Trojer, P., Mandal, S., Shilatifard, A., and Reinberg, D. (2006). Histone H2B monoubiquitination functions cooperatively with FACT to regulate elongation by RNA polymerase II. Cell *125*, 703–717.

Pokholok, D.K., Hannett, N.M., and Young, R.A. (2002). Exchange of RNA polymerase II initiation and elongation factors during gene expression in vivo. Mol. Cell *9*, 799–809.

Rozenblatt-Rosen, O., Hughes, C.M., Nannepaga, S.J., Shanmugam, K.S., Copeland, T.D., Guszczynski, T., Resau, J.H., and Meyerson, M. (2005). The parafibromin tumor suppressor protein is part of a human Paf1 complex. Mol. Cell. Biol. *25*, 612–620.

Somervaille, T.C., Matheny, C.J., Spencer, G.J., Iwasaki, M., Rinn, J.L., Witten, D.M., Chang, H.Y., Shurtleff, S.A., Downing, J.R., and Cleary, M.L. (2009). Hierarchical maintenance of MLL myeloid leukemia stem cells employs a transcriptional program shared with embryonic rather than adult stem cells. Cell Stem Cell *4*, 129–140.

Strahl, B.D., Ohba, R., Cook, R.G., and Allis, C.D. (1999). Methylation of histone H3 at lysine 4 is highly conserved and correlates with transcriptionally active nuclei in Tetrahymena. Proc. Natl. Acad. Sci. USA *96*, 14967–14972.

Sun, Z.W., and Allis, C.D. (2002). Ubiquitination of histone H2B regulates H3 methylation and gene silencing in yeast. Nature *418*, 104–108.

Szabo, J., Heath, B., Hill, V.M., Jackson, C.E., Zarbo, R.J., Mallette, L.E., Chew, S.L., Besser, G.M., Thakker, R.V., Huff, V., et al. (1995). Hereditary hyperparathyroidism-jaw tumor syndrome: the endocrine tumor gene HRPT2 maps to chromosome 1q21-q31. Am. J. Hum. Genet. *56*, 944–950.

Wade, P.A., Werel, W., Fentzke, R.C., Thompson, N.E., Leykam, J.F., Burgess, R.R., Jaehning, J.A., and Burton, Z.F. (1996). A novel collection of accessory factors associated with yeast RNA polymerase II. Protein Expr. Purif. *8*, 85–90.

Woodard, G.E., Lin, L., Zhang, J.H., Agarwal, S.K., Marx, S.J., and Simonds, W.F. (2005). Parafibromin, product of the hyperparathyroidism-jaw tumor syndrome gene HRPT2, regulates cyclin D1/PRAD1 expression. Oncogene *24*, 1272–1276.

Wu, M., Wang, P.F., Lee, J.S., Martin-Brown, S., Florens, L., Washburn, M., and Shilatifard, A. (2008). Molecular regulation of H3K4 trimethylation by Wdr82, a component of human Set1/COMPASS. Mol. Cell. Biol. *28*, 7337–7344.

Yokoyama, A., and Cleary, M.L. (2008). Menin critically links MLL proteins with LEDGF on cancer-associated target genes. Cancer Cell *14*, 36–46.

Yokoyama, A., Lin, M., Naresh, A., Kitabayashi, I., and Cleary, M.L. (2010). A higher-order complex containing AF4 and ENL family proteins with P-TEFb facilitates oncogenic and physiologic MLL-dependent transcription. Cancer Cell *17*, 198–212.

Yokoyama, A., Somervaille, T.C., Smith, K.S., Rozenblatt-Rosen, O., Meyerson, M., and Cleary, M.L. (2005). The menin tumor suppressor protein is an essential oncogenic cofactor for MLL-associated leukemogenesis. Cell *123*, 207–218.

Yu, B.D., Hess, J.L., Horning, S.E., Brown, G.A., and Korsmeyer, S.J. (1995). Altered Hox expression and segmental identity in Mll-mutant mice. Nature *378*, 505–508.

Zhang, Y., and Rowley, J.D. (2006). Chromatin structural elements and chromosomal translocations in leukemia. DNA Repair (Amst.) *5*, 1282–1297.

Zhu, B., Mandal, S.S., Pham, A.D., Zheng, Y., Erdjument-Bromage, H., Batra, S.K., Tempst, P., and Reinberg, D. (2005a). The human PAF complex coordinates transcription with events downstream of RNA synthesis. Genes Dev. *19*, 1668–1673.

Zhu, B., Zheng, Y., Pham, A.D., Mandal, S.S., Erdjument-Bromage, H., Tempst, P., and Reinberg, D. (2005b). Monoubiquitination of human histone H2B: the factors involved and their roles in HOX gene regulation. Mol. Cell *20*, 601–611.